# Concurrent Polymerization and Insertion of Aniline in Molybdenum Trioxide: Formation and Properties of a $[Poly(aniline)]_{0.24}MoO_3$ Nanocomposite

T. A. Kerr, H. Wu, and L. F. Nazar*

*Department of Chemistry, University of Waterloo, Guelph-Waterloo Centre for Graduate Work in Chemistry, Ontario, Canada N2L 3G1*

*Received February 1, 1996. Revised Manuscript Received May 6, 1996*[⊗]

We have developed a novel nanocomposite material, $[PANI]_{0.24}MoO_3$, comprised of poly(aniline) chains interleaved with the layers of $MoO_3$, using concomitant ion exchange−polymerization in the presence of an external oxidizing agent. The characterization of this material using SEM, FTIR spectroscopy, powder XRD, and thermal analysis shows that the poly(aniline) is present primarily in the emeraldine salt form. The high degree of ordering evident from the oriented film XRD patterns suggests that the PANI chains are at least partially aligned in the *ac* (basal) plane. The properties of the polymer nanocomposite for electrochemical lithium insertion were compared to those of the alkali molybdenum oxide using the materials as cathodes in conventional lithium cells. The polymer/oxide battery demonstrated substantially reduced cell polarization on galvanostatic cycling, compared to the alkali molybdenum oxide in the absence of PANI. The resultant enhanced ion and/or electron transport induced by incorporation of the polymer, in addition to the redox capacity of the intercalated PANI, provided a moderate increase in cell capacity and improved the reversibility of the Li insertion reaction.

## Introduction

Compounds that possess 3D open-framework or 2D layered structures have been investigated with much interest lately due to the unique environment for reaction offered by their vacancies. These compounds can undergo chimie douce reactions resulting in the incorporation of guest species into their structure. The synthesis of these well-ordered systems has been found to demonstrate a self-assembly process distinctive to the starting materials and conditions of the reaction. Examination of the individual components of the system and their attributes can allow chemists to design new compounds with specific, tailor-made qualities. Among these are properties involving combined ion and electron conduction.

Early studies on two-dimensional or layered compounds primarily involved the intercalation of simple, small molecules or ions into the van der Waals gap.[1] Recently, a new class of these materials has been developed based on an extension of these concepts, involving the incorporation of macromolecular species between the layers. In particular, the insertion of conjugated polymers has been examined intensively over the past few years.[2] Partial oxidation of the polymer backbone ("p-doping") provides materials that are highly conductive, and hence poses fascinating questions as to their properties upon intercalation. One question is the degree to which the polymer−polymer interactions in the bulk will be modified by substantial polymer−host interactions. These serve to sequester the polymer chains and affect either the polymer conformation, chain length, and/or bulk electron-transport properties. In addition, the possibility of electron or hole transfer between the polymer and the inorganic component exists, if the latter is a transition-metal oxide with conductive properties.[3] The application of either conjugated polymers[4] or transition-metal oxides[5] as positive electrodes in rechargeable lithium batteries and in electrochromic displays also suggests that these polymer/oxide materials, which are blended together on a "nanoscale", present new opportunities in these devices. That is, the redox capacity of the polymer can, in principle, both augment that of the oxide *and* affect lithium ion transport between the layers by virtue of propping the oxide layers further apart than in their native state.

The emeraldine salt form of poly(aniline) (PANI), is one such polymer that has been used on its own for electrochemical applications.[6] It is one of the few conductive polymers that is completely air-stable in the p-doped form and hence has been a popular component of polymer/oxide nanocomposites. Poly(aniline) has been successfully intercalated into layered structures such as zirconium phosphate $Zr(HPO_4)_2$,[7] vanadium phosphate($VOPO_4$),[8] hydrogen uranyl phosphate ($HUO_2PO_4$),[9] vanadium oxide ($V_2O_5$),[10,11] iron oxychloride

[⊗] Abstract published in *Advance ACS Abstracts,* July 15, 1996.

(1) Jacobson, A. J.; Whittingham, M. S. Intercalation Chemistry, Academic Press: New York, 1982.
(2) Ruiz-Hitzky, E. *Adv. Mater.* **1993**, *5*, 334.
(3) Day, P. *Philos. Trans. R. Soc. London A* **1985**, *A314*, 145.
(4) Bonino, F.; Scrosati, B. In *Materials for Solid State Batteries*; Chowdari, B. V. R., Radhakrishna, S., Eds.; World Scientific: Singapore, 1986; p 53.
(5) Desilvestro, J.; Haas, O. *J. Electrochem. Soc.* **1990**, *137*, 5C.
(6) Lee, J. Y.; Ong, L. H., Chuah, G. K. *J. Appl. Electrochem.* **1993**, *23*, 1031. Matsunaga, T.; Daifuku, H.; Nakajima, T., Kawagoe, T. *Polym. Adv. Technol.* **1990**, *1*, 33. Echigo, Y.; Asami, K., Takahashi, H., Inoue, K.; Kabata, T.; Kimura, O.; Ohsawa, T. *Synth. Met.* **1993**, *55*, 3611.
(7) Chao, K. J.; Chang, T. C.; Ho, S. Y. *J. Mater. Chem.*, **1993**, *3*, 427.
(8) Nakajima, H.; Matsubayashi, G. *Chem. Lett.* **1993**, 423.

S0897-4756(96)00071-3 CCC: $12.00 

(FeOCl),[12] layered double hydroxides,[13] $HTaWO_6$,[14] and molybdenum disulfide ($MoS_2$).[15] It has also been generated inside the host channel systems of zeolites such as mordenite, zeolite Y[16] and MCM-41.[17] The method for PANI insertion into each of these composites varies slightly from one host to another. Aniline undergoes concomitant intercalation and oxidative polymerization when mixed in aqueous media with highly oxidizing hosts such as $V_2O_5$, FeOCl, or layered mixed-metal ($Cu^{2+}{}_{1-x}Cr_x^{3+}$ and $Cu^{2+}{}_{1-x}Al_x^{3-}$) double hydroxides.[13] This reaction is limited to hosts that fall into a redox potential range sufficient to oxidize the monomer and also have a structure that permits the polymer to be readily inserted between the layers (a kinetic limitation). Other weakly oxidizing host structures require initial intercalation of the anilinium ion which can then be polymerized through the use of external oxidizing agents. For example, treatment with molecular oxygen has successfully polymerized anilinium in lattices which are stable under these conditions, such as $V_2O_5$[10] and layered phosphates.[7−9] Polymerization of the aniline in many cases requires 1−4 weeks for completion. $(NH_4)_2S_2O_8$ has been used to polymerize aniline in $MoO_3$, although partial dissolution of the lattice resulted from reaction with the oxidizing agent.[18] We sought an alternative method which utilized an external oxidizing agent and also benefited from the propensity of layered oxides such as $A_xMoO_3^{x-}$ (A = alkali ion) to swell in water and undergo ion-exchange reactions. We previously found, for example, that ion-exchange could be employed to insert long-chain polyelectrolytes such as the precursor to PPV, into $A_xMoO_3^{x-}$ when the layers were fully exfoliated.[19]

Here, we outline a method whereby the conductive emeraldine salt form of poly(aniline) is inserted into the van der Waals gap of semiconducting molybdenum trioxide to produce a new composite, $[poly(aniline)]_{0.24}MoO_3$. Our use of $MoO_3$ as a host is also based on studies that have shown that the reversible insertion of lithium into $MoO_3$ provides a promising rechargeable lithium battery system, albeit with some shortcomings.[20] To determine if poly(aniline) has a positive effect on lithium insertion reactions in the host lattice, we employed the polymer nanocomposite as a cathode in a conventional lithium cell. Enhancement of the electrochemical properties of $MoO_3$ by inclusion of poly(aniline) is described herein.

## Experimental Section

**Syntheses.** $[Li^+]_{0.09}[Na^+]_{0.15}(H_2O)_n[MoO_3]^{-0.25}$ ($[Li/Na]_{0.25}MoO_3$) was prepared following the literature method, substituting $Li_2MoO_4$ as the buffer in place of $Na_2MoO_4$.[21] The final material was then stored in a humid, nitrogen atmosphere to prevent degradation and/or dehydration. For use in battery experiments, the alkali bronze was thrice exchanged with LiI for 5 h each time in a 1.0 M solution of *n*-butanol. The material was filtered, washed thoroughly with *n*-butanol, and stored under a dry nitrogen atmosphere. Dehydration under vacuum for 24 h at 100 °C yielded a material of stoichiometry $[Li_{0.8}Na_{0.2}\ 0.5H_2O]_{0.25}MoO_3$ ("$Li_{0.25}MoO_3$"). This procedure was devised to maximize the Li/Na ratio. The "fully" Li-exchanged material did not, however, display a significant difference in battery performance compared to the mixed alkali bronze $[Li/Na]_{0.25}MoO_3$.

$[Poly(aniline)]_xMoO_3$ ($[PANI]_{0.24}MoO_3$) was prepared by adding excess aniline (4 mL) to a sonicated suspension of 50 mg $[Li/Na]_{0.25}MoO_3$ in 20 mL of deionized water. For the deuterium NMR studies, perdeuterated aniline (98 atom % D; Cambridge Isotope Laboratories) was substituted for the aniline. The suspension was stirred for 30 min to ensure complete mixing. The oxidizing agent, iron(III) chloride (2 equiv) was then added to the solution. After 10 min, 20 mL of *n*-butanol was added and the reaction was stirred for 30 min. The product was separated from the aqueous solution, washed with *n*-butanol, and collected by centrifugation. For molecular weight determinations, PANI was extracted from the $[PANI]_{0.24}MoO_3$ composite by dissolving the latter in dilute NaOH, and adding 1 M HCl to precipitate the emeraldine salt form of the PANI, which was then collected by centrifugation. The extracted PANI was treated with base to convert the polymer salt to the soluble base form. To serve as a "reference" material, emeraldine base/salt was prepared according to the literature method.[22]

**Gel Permeation Chromatography.** Molecular weight determinations were performed at 25 °C using a Waters Chromatographic System equipped with a 500 mm Jordi linear mixed-bed column. A filtered (1 $\mu$m Millipore) 100 $\mu$L injection charge of $4 \times 10^{-4}$ g/mL of the extracted emeraldine base in NMP was used and eluted with 0.5% (w/w) LiCl/N-methyl-2-pyrrolidone (NMP) at a flow rate of 0.5 mL $min^{-1}$. The UV−vis detector was set at 315 nm for PANI, and a differential refractive index detector was used for the polystyrene standards. The weight and number-average molecular weights ($\bar{M}_w$ and $\bar{M}_n$, respectively) were calculated from a calibration curve of monodisperse poly(styrene) (PS) standards ranging from 2100 to 575 000. We emphasize that all GPC weights for PANI are "apparent" molecular weights, since the calibration was performed using polystyrene.

**Instrumentation.** X-ray powder diffraction (XRD) patterns were obtained on a Siemens D500 X-ray diffractometer equipped with a diffracted beam monochromator, using Cu Kα radiation. Samples were prepared by evaporating suspensions of the intercalated oxide onto microscope slides. This resulted in preferred orientation of the oxide layers parallel to the plane of the slide, which therefore selectively enhanced the interlayer (or 0*k*0) diffraction peaks, and suppressed the mixed *hkl* or *h*0*l* diffraction peaks. Samples were scanned at a step scan rate of 0.02°/s. Infrared spectra were recorded on a Nicolet 520 FTIR as KBr pellets. The $^2H$ NMR spectrum was obtained at 11.7 T at a frequency of 76.7 MHz on a Bruker AMX-500 with complete solid-state accessories using a high-power wideline probe with a 5 mm diameter solenoidal coil; typical 90° pulse lengths were 2.4 $\mu$s. A standard quadrupole echo pulse sequence with an interpulse delay of 30 $\mu$s and a recycle delay of 5 s was applied and a first pulse of 30° was used to attain more uniform excitation across the broad spectrum. Differential thermal analysis and thermal gravimetric analysis (DTA/TGA) were performed on a PL Thermal Sciences STA

(9) (a), Liu, Y.-J.; Kanatzidis, M. G. *Inorg. Chem.* **1993**, *32*, 2989. (b) Liu, Y.-J.; Kanatzidis, M. G. *Chem. Mater.* **1995**, *7*, 1525.
(10) Liu, Y.-J.; DeGroot, D. C.; Schlindler, J. L.; Kannewurf, C. R.; Kanatzidis, M. G. *J. Chem. Soc., Chem. Commun.* **1993**, 593.
(11) Kanatzidis, M. G.; Wu, C. *J. Am.. Chem. Soc.* **1989**, *111*, 4139.
(12) Kanatzidis, M. G.; Wu, C. G.; Marcy, H. O.; DeGroot, D. C.; Kannewurf, C. R.; Kostikas, A.; Papaefthymiou, V. *Adv. Mater.* **1990**, *2*, 364.
(13) Challier, T.; Slade, C. T. *J. Mater. Chem.* **1994**, *4*, 367.
(14) Koene, B.; Nazar, L. F. *Solid State Ionics*, in press.
(15) Kanatzidis, M. G.; Bissessur, R.; DeGroot, D. C.; Schindler, J. L.; Kannewurf, C. R. *Chem. Mater.* **1993**, *5*, 595.
(16) Enzel, P.; Bein, T. *J. Phys. Chem.* **1989**, *93*, 6270.
(17) Wu, C.-G.; Bein, T. *Science* **1993**, *264*, 1757.
(18) Bissessur, R.; DeGroot, D. C.; Kanatzidis, M. G.; Schindler, J. L.; Kannewurf, C. R. *J. Chem. Soc., Chem. Commun.* **1993**, 687.
(19) Nazar, L. F.; Zhang, Z.; Zinkweg, D. *J. Am. Chem. Soc.* **1992**, *114*, 6239. Nazar, L. F.; Yin, X. T.; Zinkweg, D.; Zhang, Z.; Liblong, S. *Mater. Res. Soc. Symp. Proc.* **1991**, *210*, 417.
(20) (a) Nazri, G. A.; Julien, C. *Solid State Ionics* **1994**, *68*, 111. (b) Julien, C.; Nazri, G. A.; Gorenstein, J. P.; Khelfa, A.; Hussain, O. M. *Solid State Ionics* **1994**, *73*, 319.
(21) Thomas, D. M.; McCarron, E. M. *Mat. Res. Bull.* **1986**, *21*, 945.
(22) MacDiarmid, A. G.; Change, J. C.; Richter, A. F.; Somasiri, N. L. D.; Epstein, A. J. *Conducting Polymers*, Alcacer, L., Ed.; Reidel Publishing Co: Holland 1987, p 105.

**Scheme 1. Schematic Diagram of the Swelling and Reassembly Process for the Preparation of $[PANI]_{0.24}MoO_3$**

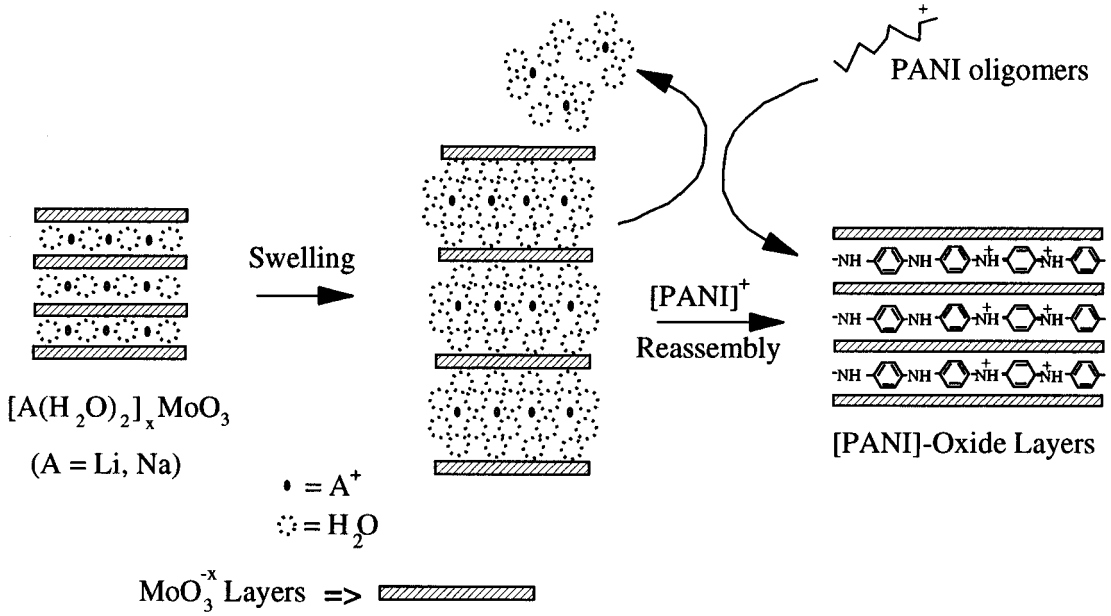


1500 thermal analysis system (when it was working). DTA and TGA curves were run simultaneously on each sample from room temperature to 500 °C in a flowing atmosphere of air using a heating rate of 5 °C/min. Variable-temperature conductivity measurements were performed using a four-probe method in a vacuum chamber with a pressure lower than $10^{-4}$ Torr. Gold wire electrodes were affixed to the sample using conductive gold paste, and the sample was heated-treated at 120 °C in vacuum to cure the epoxy.

**Electrochemical Measurements.** The electrochemical properties were examined using a "Swagelock-type" cell comprised of a Teflon (or Delrin) outer housing fitted with inner screw threads. Stainless steel posts tightly threaded into either end of this assembly thereby functioned as the two external electrodes. A circular disk of metallic Li comprised the anode. The electrolyte was composed of anhydrous $LiClO_4$, dried under vacuum at 180 °C for 24 h, and dissolved to make a 1.0 M solution in propylene carbonate (PC, Aldrich). The PC was twice vacuum distilled over molecular sieves prior to use. Glass-fiber paper soaked with electrolyte was used as the separator in the cells. The working electrode consisted of approximately 5 mg of the desired polymer/oxide nanocomposite, or $Li_xMoO_3$ mixed with 20% (by weight) carbon black and either poly(vinylidene fluoride) (PVDF) or EPDM (ethylene propylene diene monomer) as the binder. The mixture was pressed onto a stainless steel mesh grid, and the cathode pellet was dried under vacuum for 48 h at 80 °C. The cells were charged and discharged in an argon atmosphere at a constant current density of 60 $\mu$A/cm$^2$ between preset voltage limits using a multichannel galvanostat/potentiostat system (Macpile).

## Results and Discussion

**A. Structure and Characterization.** Inorganic oxides rarely exhibit layered structures that are stable in the absence of interlayer cations, due to structural instability caused by electrostatic repulsion of the electronegative oxide ions on neighboring layers. $MoO_3$, however, is one exception. The structure consists of vertex-sharing chains of distorted $MoO_6$ octahedra which share edges with two similar chains to form layers. The distortion gives rise to very short "Mo=O" bonds at the apical octahedral positions, that terminate the top and bottom of the double-octahedral oxide sheets. The resultant two-dimensionally bonded layers are stacked in a staggered arrangement and held together by weak van der Waals forces. A variety of large guest species can be intercalated into the interlayer van der Waals gap (albeit with some difficulty). Unlike more oxidizing transition-metal oxides such as $V_2O_5$, however, the electrochemical redox potential of $MoO_3$ (3.2 V) is not sufficient to oxidatively polymerize monomers such as aniline, bithiophene, and pyrrole during the insertion reaction. Hence, we sought to develop another technique that could be used to insert conductive polymers between the layers of relatively "redox-inert" oxides. Our method employs a combination of methods that involves first swelling apart the $MoO_3$ layers, followed by concomitant ion exchange and oxidative polymerization by an external oxidizing agent. The concept is summarized in Scheme 1 that illustrates a polymer intercalation process that begins with the expansion of the $MoO_3$ layers upon cation solvation.

To swell the layers apart, we chemically reduced the molybdenum oxide to form the hydrated lithium/sodium molybdenum bronze, $[Li^+(H_2O)_n]_x[Na^+(H_2O)_m]_y[MoO_3]^{x+y}$ ($[Li/Na]_{0.25}MoO_3$ where both $n$ and $m$ depend on the drying history of the sample). The interlayer alkali-metal cations are important in facilitating the dispersion of the oxide layers during intercalation, since the extent of the layer exfoliation is dependent on the alkali-metal cations initially present in the bronze. The effect of the alkali was probed by preparing four different oxide bronzes with differing ion ratios: (I) Li/Na = 0.5; (II) Li/Na = 0.7; (III) Li/Na = 1.5; (IV) Li/Na = 3.3. Bronze I was prepared by reaction of $MoO_3$ with $Na_2S_2O_4$, except that $Li_2MoO_4$ acted as the buffer. The Li content in the other bronzes was increased by sequential ion-exchange of I with 1.0M LiI, for a period of 5 h at each step, with II, III, and IV corresponding to one, two, and three exchange steps, respectively. We found that the optimum Li/Na ratio to achieve well-ordered materials was between 0.5 and 1.0. This is due to the greater hydration energy of $Li^+$ versus that of $Na^+$. It gives rise to a small degree of interlayer swelling by water when the Li/Na ion ratio is zero (monolayer of water, Figure 1a), intermediate swelling at higher Li/Na ratios, <0.5

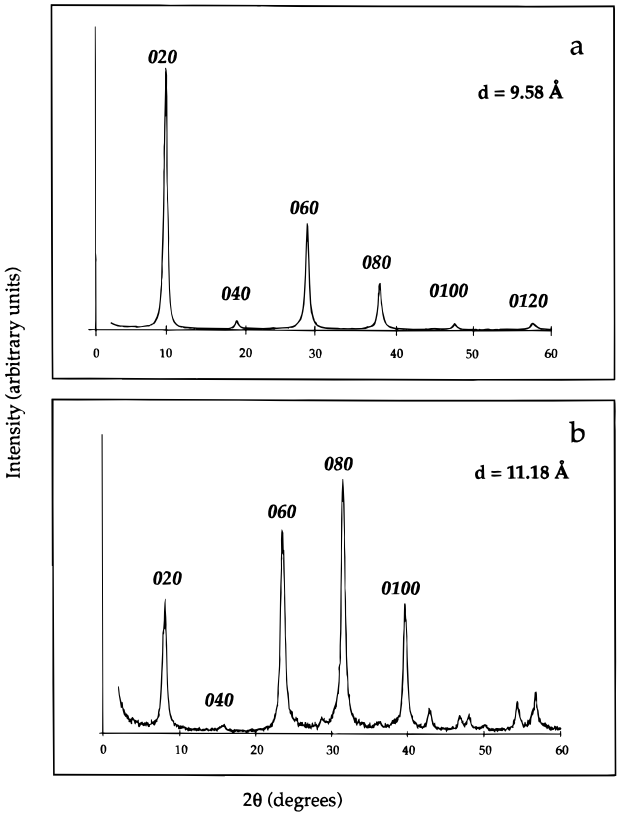


**Figure 1.** XRD patterns of (a) partially hydrated $[Li/Na(H_2O)_2]_{0.25}MoO_3$ and (b) fully hydrated $[Li/Na(H_2O)_5]_{0.25}MoO_3$.

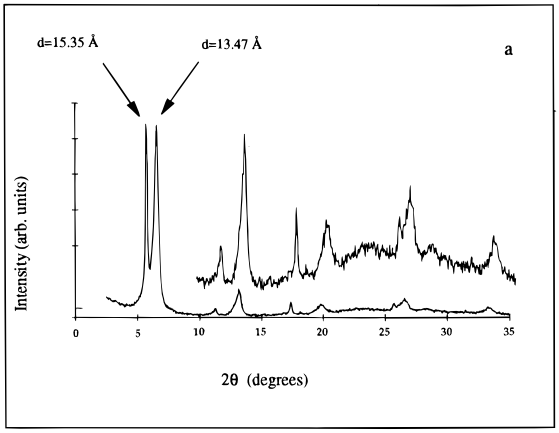


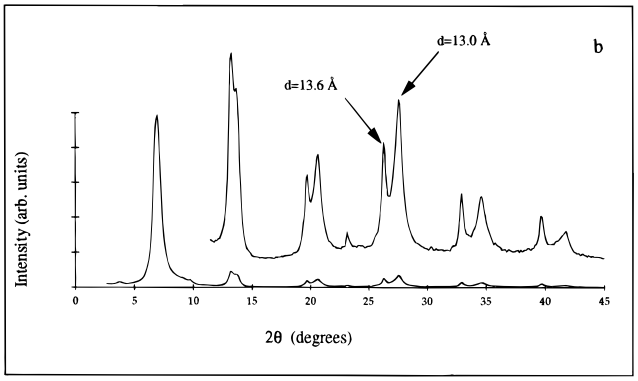


**Figure 2.** Effect of (a) heat and (b) excess $FeCl_3$ on the crystallinity of $[PANI]_{0.24}MoO_3$.

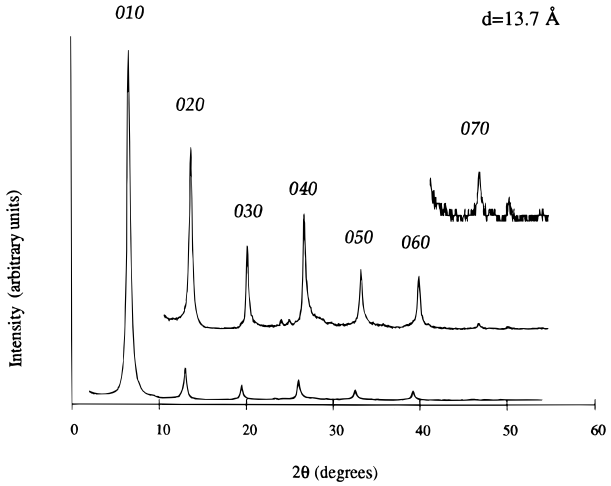


**Figure 3.** XRD pattern of $[PANI]_{0.24}MoO_3$ prepared using a 30 min reaction period.

(bilayer of water, Figure 1b), but a very large degree of swelling when the Li/Na ratio is larger than 1.0. Formation of the poly(aniline)/$MoO_3$ nanocomposite was effected by reacting the $[Li/Na]_{0.25}MoO_3 \cdot H_2O$ bronze (Li/Na $\approx$ 0.7) with aniline in the presence of $FeCl_3$. This reaction probably proceeds *via* ion-exchange of the interlayer alkali ions with oligo- or polymeric, positively charged aniline units that are generated by oxidative polymerization.

Our experiments have shown that multiphase products can be obtained by altering the reaction conditions. A two-phase product (corresponding to materials with interlayer *d* spacings of 13.7 and 13.0 Å) results from the use of excess $FeCl_3$ (Figure 2b). The two distinct interlayer distances probably correspond to different conformations or degrees of protonation of the polymer chains between the layers. When the reaction was carried out at 60 °C, a two-phase mixture also resulted. The XRD pattern of this two-phase mixture is shown in Figure 2a with the two phases at 15.35 and 13.47 Å identified by their 0*k*0 reflections. The low crystallinity of this sample is demonstrated by the broad, low-intensity reflections. The appearance of the two distinct interlayer spacings suggests again that the poly(aniline) chains have adopted two different conformations or orientations between the $MoO_3$ layers. The most highly crystalline, single phase product ($d$ = 13.67 Å) was obtained using reaction times of 0.5 h. Substantial oxidation of the molybdenum trioxide occurs when reaction times of over 4 h are used. Reaction times shorter than 0.5 h lead to a two-phase mixture of the 13.7 Å phase and the$[Li/Na]_xMoO_3$ phase; the latter gradually disappears as the reaction progresses, suggesting that it originates from larger crystallites or incompletely swelled starting material. Changing the order of reactant addition during the synthesis also affected the crystallinity of the final product. The most completely exchanged, well-ordered materials were obtained by forming a suspension of the oxide bronze in water and then sequentially adding the aniline, the oxidizing agent, and butanol.

The XRD pattern for the single phase product $[PANI]_x$-$MoO_3$ favored at ambient temperatures and moderate amounts of $FeCl_3$ is shown in Figure 3. An average *d* spacing of 13.67 Å was calculated from the nine 0*k*0 reflections. The 6.8 Å increase in *d* spacing from 6.93 to 13.67Å is consistent with intercalation of the poly(aniline) into the $MoO_3$ sheets in a helical chain conformation or with the phenyl rings lying roughly per-

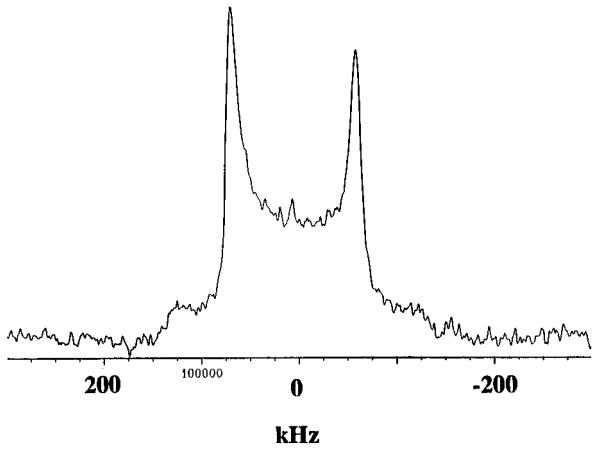


**Figure 4.** Quadrupolar echo $^2$H spectrum of $[PANI]_{0.24}MoO_3$ at 298 K, acquired with a repetition delay of 5 s, number of scans = 512, $\tau = 30$ $\mu$s.

pendicular to the layers, similar to the case of the poly(*p*-phenylenevinylene)$MoO_3$ composite.[19] Samples that had been left standing at ambient temperatures for several days retained their crystallinity, showing no deviations in their XRD patterns from those of freshly made materials. The solid-state $^2$H NMR spectrum of deuterated $PANI_xMoO_3$ is shown in Figure 4. The observed splitting of the Pake doublet (124 kHz) is typical of that of completely static phenyl deuterons such as those found in confined enviroments[23] and indicates that the polymer chains are rigidly confined between the oxide layers at room temperature. In fact, the line shape and spectral parameters ($\eta \sim 0$; NQCC $\sim$ 165 kHz) are very similar to those observed for bulk PANI emeraldine salt, for which the fraction of rings undergoing 180° flips was also insignificant at ambient temperature and much less (about 35%) that of the emeraldine base.[24] Here, the static nature of the polymer can be attributed to a combination of strong interaction with the $MoO_3^{x-}$ layers and its electronic structure.

Characterization of other nanocomposites have shown that the interlayer distances are consistent with the interstitial PANI chains being oriented with the planes of the phenyl rings perpendicular to the layers.[11,13,25] This was not the case when poly(aniline) was intercalated between the layers of $MoS_2$. For this composite, the poly(aniline) chains were found to be oriented with the phenyl rings lying parallel to the metal sulfide layers resulting in a 4.2Å interlayer expansion.[15] In our $PANI_xMoO_3$, a high degree of ordering along the axis perpendicular to the layers is evident from the intense sharp peaks that are obtained and the small variation in $d_{0k0}$ (±0.03 Å). These results suggest that the polymer chains are not entangled but rather lie parallel to each other in the "valleys" or "troughs" of the oxide sheets. This high degree of ordering has also been observed in the poly(phenylene vinylene)$MoO_3$ composite[19] but is absent in the polypyrrole−$MoO_3$ (PPY−$MoO_3$) composite.[26] This is probably due to the difference in the polymer crystallinity, and the possibility of α,β-coupling in the formation of the PPY polymer;[27] i.e., PPV and PANI are significantly more ordered than PPY. The relatively low level of crystallinity of PPY−$MoO_3$ may also be due to a nondescript orientation adopted by the polymer between the $MoO_3$ layers. By comparison, the high crystallinity of the PANI and its specific orientation between the oxide layers influences the overall crystallinity of the composite. Scanning electron micrographs of both the lithium sodium molybdenum bronze and the intercalated polymer product show the sheet stacking of the microcrystallites platelets (Figure 5). It is evident that the incorporation of PANI into the $MoO_3$ does not result in a reduction of crystallite size (or increase in surface area); it is also evident that there are no large bulk deposits of polymer on the surface of the crystallites, although small amounts of PANI on the surface would be impossible to detect by SEM.

**Table 1. Elemental Analysis Results for $[PANI]_xMoO_3$ (Guelph Chemical Laboratories, Guelph, Canada)**

| sample | Mo (wt %) | C (wt %) | N (wt %) | Na, Li (wt %) | *x* in $[PANI]_xMoO_3^{x-}$ |
|---|---|---|---|---|---|
| 1A | 49.60 | 8.95 | 1.56 | ND[a] | 0.236 |
| 1B | 49.45 | 8.62 | 1.72 | ND | 0.233 |

[a] ND = not detected.

The results of elemental analysis are summarized in Table 1, verifying that there is no lithium or sodium present in the final product. Therefore, the interlayer alkali ions present initially in the bronze are completely replaced by the intercalated polymer. The average polymer/oxide stoichiometry of the material ($[PANI]_{0.24}MoO_3$) is in good accord with theoretical estimates of the polymer content. Our calculations based on the length of an aniline monomer unit (5.7 Å) and the basal (*ac*) cell dimensions of $A_xMoO_3$ (3.733 Å × 3.876 Å)[21] yield an upper limit theoretical stoichiometry of $[PANI]_{0.33}MoO_3$, assuming that a poly(aniline) chain occupies each "trough" in the lattice. However, the single-crystal structure of the emeraldine salt form of the PANI tetramer indicates that it adopts a helical conformation with a dihedral angle of +15.3° and −15.3° alternating between nitrogen atoms.[28] Using this as a structural model, the resulting PANI structure resembles more that of a cylinder rather than a flat plane. Our modeling studies using Cerius$^2$ established that this is the most stable conformation of PANI, and furthermore suggested that this conformation could not be supported in every trough of the $MoO_3$ but only in every *other* trough, resulting in a stoichiometry of $[PANI]_{0.19}MoO_3$ (Figure 6). Our experimental composition is closer to this predicted stoichiometry; however, more extensive modeling studies are currently underway to confirm this hypothetical structure since the PANI conformation may be strongly affected by interaction with the $MoO_3$ lattice. We note that Kanatzidis et al. have also briefly described the inclusion of $PANI^+$ in $MoO_3$ using a different route.[18] Their synthesis yielded a final product with a stoichiometry of $[PANI]_{0.7}MoO_3$. The high ratio of PANI to $MoO_3$ (0.7) was reported to be a result of partial

(23) Spiess, H. W. In *Advances in Polymer Science 66*; Kausch, H. H., Zachmann, H.G., Eds.; Springer-Verlag: Berlin, 1985.
(24) Kaplan, S.; Conwell, E. M.; Richter, A. F.; MacDiarmid, A. G. *Macromolecules*, **1989**, *22*, 1669.
(25) Liu, Y.-J.; DeGroot, D. C.; Schindler, J. L.; Kannewurf, C. R.; Kanatzidis, M. G. *Adv. Mater* **1993**, *5*, 369.
(26) Wu, H.; Nazar, L. F.; submitted.
(27) Saunders, B. R.; Fleming, R. J.; Murray, K. S. *Chem. Mater.* **1995**, *7*, 1082.
(28) Shacklette, L. W.; Wolf, J. F.; Gould, S.; Baughman, R. H. *J. Chem. Phys.* **1988,** *88*, 3955. Baughman, R. H.; Wolf, J. F.; Edkhardt, H.; Shacklette, L. W. *Synth. Met.* **1988**, *25*, 121.

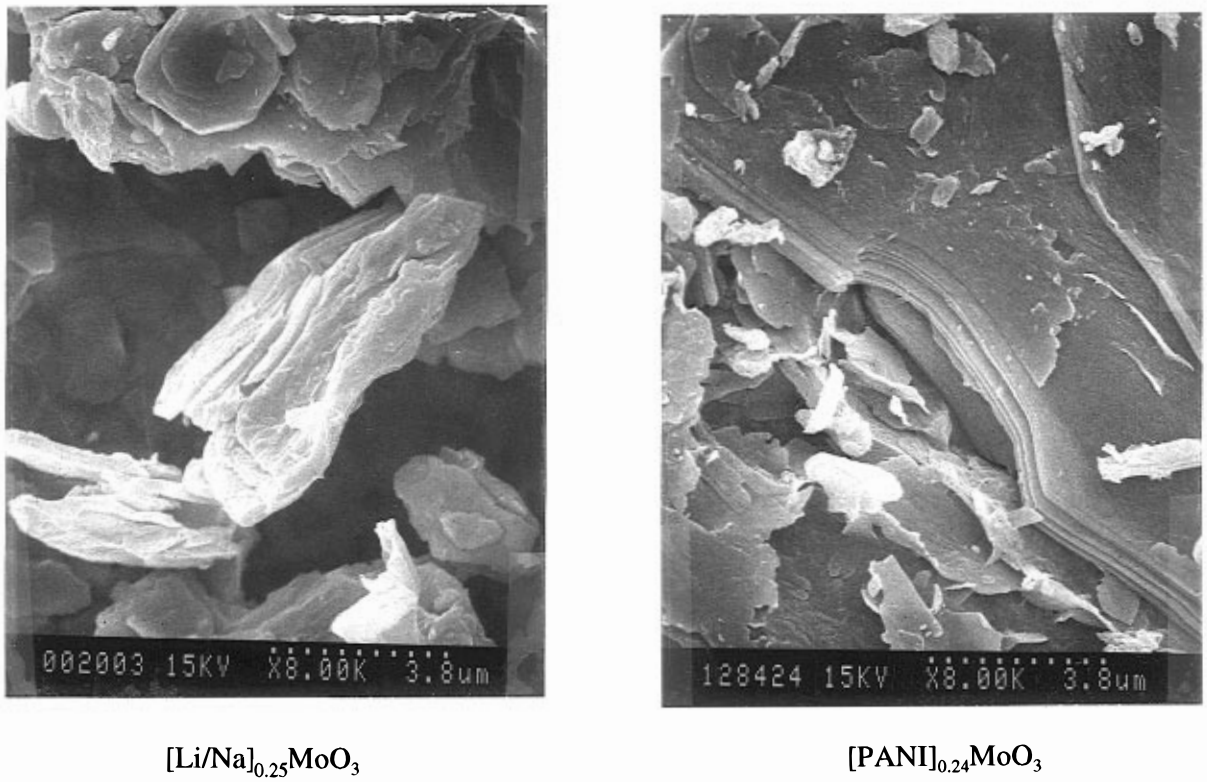


**Figure 5.** SEM micrographs of $[Li/Na]_{0.25}MoO_3$ and $[PANI]_{0.24}MoO_3$.

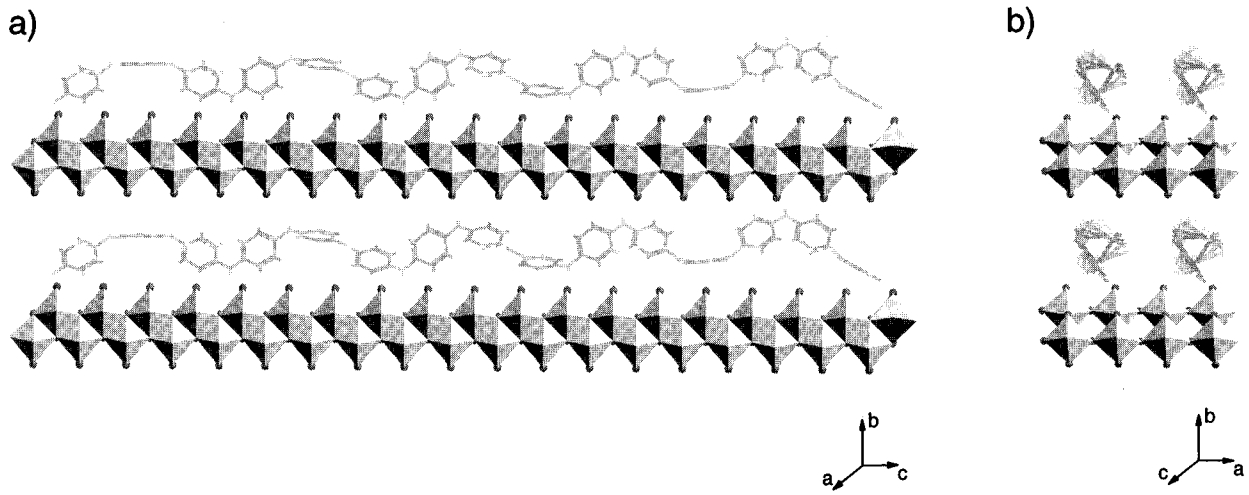


**Figure 6.** Possible ordering of poly(aniline) chains in every other "trough" of the $MoO_3$ lattice: (a) view along [100]; (b) view along [001].

dissolution of the oxide by the $(NH_4)_2S_2O_8$ oxidizing agent.

**FTIR.** Figure 7 shows the IR spectra of $[PANI]_{0.24}MoO_3$ (lower trace), along with the IR spectra of $[Li/Na]_{0.25}MoO_3$, the emeraldine base form of PANI, and the emeraldine salt form of PANI for comparison. The 1500−500 $cm^{-1}$ region of the infrared spectrum is sensitive to C−H vibrations. Shifts in this region can be used to identify changes in the polymer structure. Owing to the longer conjugation lengths in the salt, the vibrational bands of the base at 1596, 1502, 1167 and 831 $cm^{-1}$ are shifted to 1581, 1494, 1153, and 807 $cm^{-1}$ after doping with HCl. These peaks also become broader and change in relative intensity as a result of the increased oscillations of the backbone from the resonant coupling with the charge fluctuation along the chain.[29] The most prominent change in the infrared spectra of these two PANI forms is the 1167 $cm^{-1}$ band that intensifies, broadens, and shifts upon doping.[29] A unique characteristic absorption is also found from 4000 to 1600 $cm^{-1}$ in the IR spectrum of emeraldine salt. This broad and intense absorption is due to the free-charge carrier absorption in the conductive polymer.[28]

Comparison of the $PANI_{0.24}MoO_3$ spectrum with that of poly(aniline) indicate that it is primarily the emeraldine salt form that is present in our composite. This conclusion is based on the presence of a broad, intense free-charge carrier absorption band at high wavenumber and the presence of a band at 1150 $cm^{-1}$. This peak is broad and rounded just as in the salt spectrum and

(29) Wang, Y.; Rubner, M. F. *Synth. Met.* **1992**, *47*, 255.

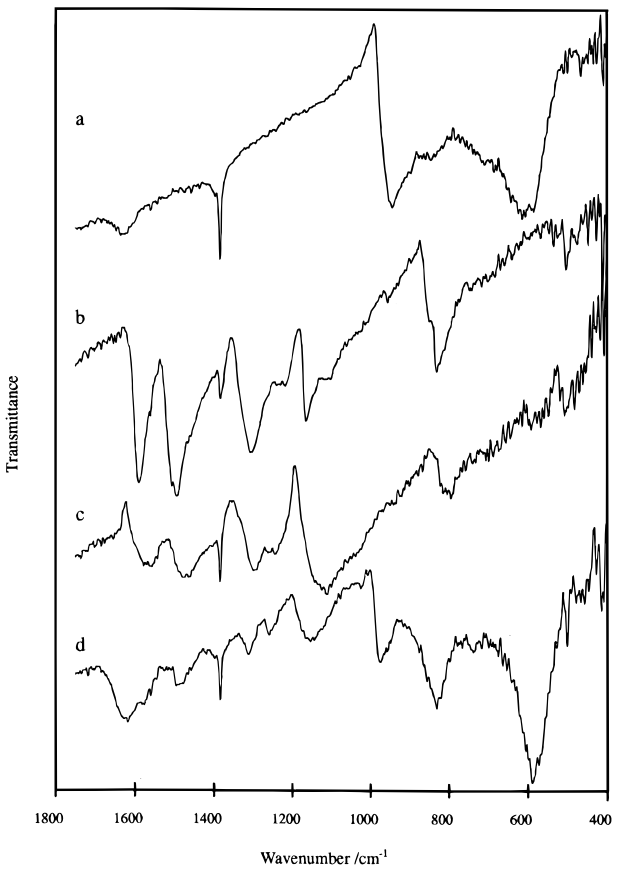


**Figure 7.** FTIR spectra of (a) $[Li/Na]_{0.25}MoO_3$, (b) PANI emeraldine base, (c) PANI emeraldine salt, and (d) $[PANI]_{0.24}MoO_3$.

**Table 2. FTIR Spectral Assignments for $[poly(aniline)]_{0.24}MoO_3$**

| frequency ($cm^{-1}$) | assignment | ref |
|---|---|---|
| 1614 | quinoid phenyl ring breathing mode; $\nu$(C═C) | 13, 42 |
| 1486 | benzenoid phenyl ring breathing mode; n(C═C) | 13, 34 |
| 1310 | quinoid−benzenoid−quinoid $\nu$(C−N) | 43, 44 |
| 1258 | aromatic $\nu$(C−N) | 34 |
| 1150 | para-substituted aromatic $\delta$ (C−H in plane) | 13, 35 |
| 970 | symmetric stretching vibration $\nu$(Mo═O) | 45, 46 |
| 832 | para-substituted aromatic $\delta$ (C−H out-of-plane) | 47 |
| | $\nu$(Mo−O−Mo) | 48 |
| 586 | $\nu$(Mo−O) | 36 |

shows obvious contrast to the sharp 1167 $cm^{-1}$ peak of the base. The spectrum, however, also reveals a band at 830 $cm^{-1}$, close to that observed in the emeraldine base spectrum. This suggests that the PANI chains in the $MoO_3$ may exist in both the salt and the base form. The overall character of the $[PANI]_{0.24}MoO_3$ spectrum looks more like the salt than the base spectrum, suggesting that base form of PANI is present only in small proportions. The IR assignments are summarized in Table 2. Comparison of the $[PANI]_{0.24}MoO_3$ spectrum with the $[Li/Na]_{0.25}MoO_3$ spectrum also confirms that the $MoO_3$ has remained in a reduced state. Our studies show that when $MoO_3$ is reduced, the crystal symmetry changes such that only two broad absorptions are visible in the spectrum.[30]

**Thermal Analysis.** Figure 8a shows the thermal gravimetric and differential thermal analysis curves of the poly(aniline) intercalated molybdenum trioxide

(30) Zhouyao, Z.; M.Sc. Thesis, University of Waterloo, 1991.

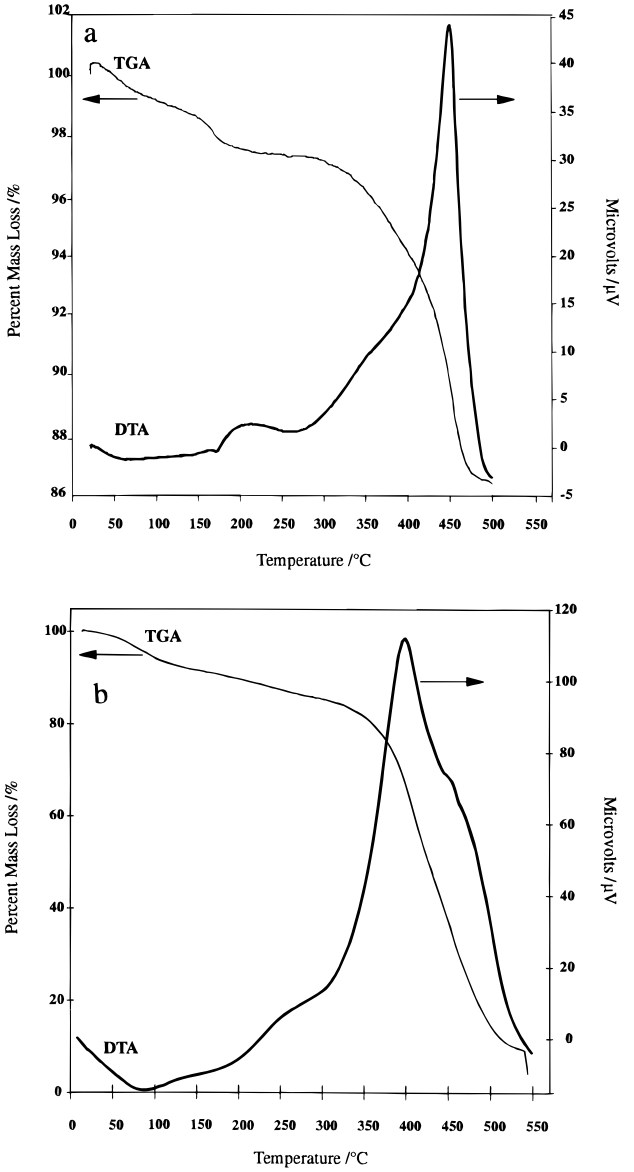


**Figure 8.** (a) TGA/DTA curves of $[PANI]_{0.24}MoO_3$ composite. (b) TGA/DTA curves of emeraldine salt.

sample. The DTA curve shows a large, relatively sharp exotherm at ~425 °C due to the degradation/oxidation of the poly(aniline) between the layers. This correlates with the DTA of bulk emeraldine salt which shows a broader exotherm at 400 °C (Figure 8b). The narrow width of the exothermic transition implies a narrow molecular weight distribution of the PANI within the layers, which was confirmed by molecular weight measurements (vide infra, following section). The 13% weight loss corresponds to a stoichiometry of $[PANI]_{0.28}MoO_3$, in good agreement with that determined by chemical analysis ($[PANI]_{0.24}MoO_3$). Subsequent preparations of the nanocomposite yielded essentially the same stoichiometry, within a range $[PANI]_{0.22-0.28}MoO_3$. We attribute the small endotherm in Figure 8a at 180 °C to the loss of residual interlayer aniline or aniline oligomers (1% weight loss) near the crystallite edges. The latter temperature is too high to be assigned to water loss, which occurs at about 120 °C in the layered alkali bronzes.[21] The origin of the small exothermic event at 220 °C is not known, but may be due to the polymerization of residual aniline or aniline oligomers within the material, or a phase transition. The results

confirm that poly(aniline) is the species present in the intralamellar space and not aniline or the anilinium ion. We have previously shown that when interlayer anilinium is heated in air, an exotherm corresponding to the polymerization process is observed with no associated weight loss.[14] The TGA is also in accordance with the SEM data that show no bulk polymer are present on the surface of the $MoO_3$. When surface poly(aniline) is present, an independent exotherm corresponding to its oxidation occurs at a temperature lower than for intercalated poly(aniline).

**Molecular Weight Determination of PANI.** For the emeraldine base form of PANI that was extracted from the $MoO_3$ lattice, we found that only 10−20% of the PANI would dissolve in NMP; hence, a substantial portion of the PANI is insoluble due to its high molecular weight, cross-linking, or both.[31] The portion that did dissolve displayed a unimodal, but slightly asymmetric elution curve. Calculation of the weight ($\bar{M}_w$) and number average ($\bar{M}_n$), and polydispersity index (PDI) for the extracted PANI gave values of $\bar{M}_w = 3900$, $\bar{M}_n = 2400$, PDI = 1.6; these $\bar{M}_n$ spanned a range from 2 100 to 36 600. For chemically synthesized PANI the corresponding values were $\bar{M}_w = 58\,400$, $\bar{M}_n = 16\,300$, PDI = 3.6, typical of those of bulk PANI.[32] The molecular weights for the extracted PANI are much lower, in accordance with the results from other PANI/layered oxide nanocomposite materials.[9b,18,33] This is undoubtedly due to the confining enviroment provided by the inorganic lattice during polymerization, as others have speculated. The extracted PANI chains are, on average, shorter than that reported by Kanatzidis et al. for the $[PANI]_{0.7}MoO_3$ composite ($\bar{M}_w = 24\,200$, $\bar{M}_n = 4850$).[18] This difference may be due to exposure of the polymer during partial dissolution of the lattice in that case and/or the influence of the chemical polymerization conditions on the properties of the PANI. Specifically, we used a higher reaction temperature during the oxidation stage (25 vs 0 °C)[34] and a different oxidizing agent ($FeCl_3$ vs $(NH_4)_2S_2O_8$).[35] Both factors are known to shorten the chain-length of the PANI. The change in reaction conditions, however, also results in a much narrower chain length (PDI = 1.6) distribution than that reported for $[PANI]_{0.7}MoO_3$ (PDI = 5.0).[18] All of the polymerization variables, on the other hand, are strikingly similar to those reported for PANI formation by atmospheric oxidation of aniline in layered titanium/zirconium/uranium phosphates.[9b]

**Conductivity.** Variable-temperature dc conductivity data (four probe) on polycrystalline thin films of $[PANI]_{0.24}MoO_3$ show a linear decrease in conductivity as a function of decreasing temperature, indicative of thermally activated electron transport with an activation energy of 0.2 eV (Figure 9). Similar behavior was also observed for $PPV_{0.3}MoO_3$, for which an activation energy of 0.2 eV was also determined.[19,30] These results

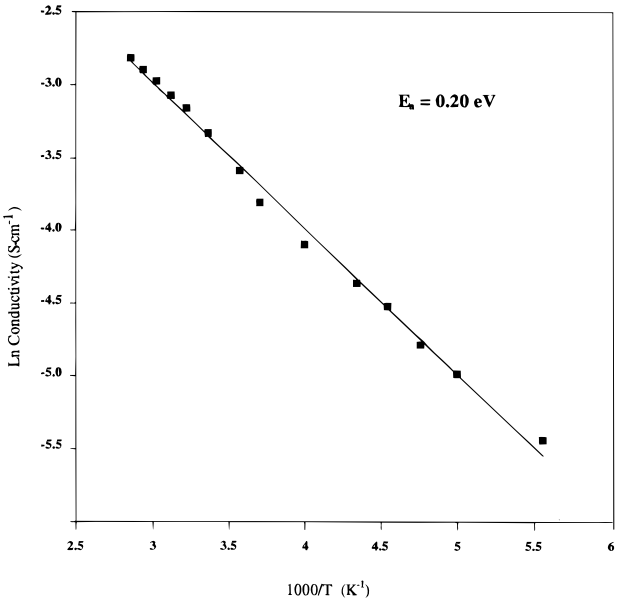


**Figure 9.** Variable-temperature four-probe conductivity data for $[PANI]_{0.24}MoO_3$.

**Table 3. Room-Temperature Conductivities of Inorganic−PANI Nanocomposites (from Refs 7−12)**

| poly(aniline) host material | room-temp conductivity (S cm$^{-1}$) |
|---|---|
| $ZrPO_4$ | $3 \times 10^{-4}$ |
| $HUO_2PO_4$ | $<1 \times 10^{-10}$ |
| $V_{2O5}$ | $5 \times 10^{-3}$ |
| $MoS_2$ | 0.4 |
| zeolite Y | $<1 \times 10^{-8}$ |
| FeOCl | $7 \times 10^{-3}$ |

can be compared to those of single-crystal conductivity measurements of hydrogen molybdenum bronzes, $H_xMoO_3$. Surprisingly, at a similar level of reduction to the nanocomposite ($H_{0.5}MoO_3$) the activation energy is 0.4 eV, (although it decreases to 0.19 eV for the more highly reduced $H_{1.7}MoO_3$).[36]

The room temperature conductivity for the $[PANI]_{0.24}MoO_3$ composite was $5 \times 10^{-4}$ S cm$^{-1}$, within the range of other poly(aniline) nanocomposites ($10^{-5}$−$10^{-2}$ S cm$^{-1}$) for which the room-temperature conductivities are given in Table 3. Pristine molybdenum trioxide is an insulator with a room-temperature conductivity of $5 \times 10^{-11}$ S cm$^{-1}$.[37] The conductivity of $[PANI]_{0.24}MoO_3$ is therefore substantially increased over that of pristine $MoO_3$, and is higher compared to polycrystalline thin films of $Na_{0.25}MoO_3$ which show room-temperature values of about $1 \times 10^{-4}$ S cm$^{-1}$. It is, not surprisingly, lower than that of bulk emeraldine salt (∼1 S cm$^{-1}$). It is also slightly lower than the value reported for $[PANI]_{0.7}MoO_3$, $3 \times 10^{-3}$ S/cm, which may reflect the difference in measurement method (thin film vs pressed pellet); the differences in PANI chain length and/or the oxidizing agent used to polymerize the aniline; and more probably, the PANI content/location in the two materials (vide supra). With respect to the latter, Kanatzidis et al. have shown that for $[PANI]_xV_2O_5$, prepared by reaction of aniline with $H_xV_2O_5$, that the conductivity

(31) Geniès, E. M.; Noël, P. *Synth. Met.* **1992**, *46*, 285.
(32) Hsu, C.-H.; Peacock, P. M.; Flippen, R. B.; Manohar, S. K.; MacDiarmid, A. G.; *Synth. Met.* **1993**, *60*, 233.
(33) Wu, C. G.; DeGroot, D. C.; Marcy, H. O.; Schindler, J. L.; Kannewurf, C. R.; Bakas, P. V.; Hirpo, W.; Yesinowski, J. P. T.; Liu, Y.-J.; Kanatzidis, M. G. *J. Am. Chem. Soc.* **1995**, *117*, 9229.
(34) Abe, M.; Ohtani, A.; Unemoto, Y.; Akizuki, S.; Ezoe, M.; Higuchi, H.; Nakamoto, K.; Okumo, A.; Noda, Y. *J. Chem. Soc., Chem. Commun.* **1989**, 1736.
(35) Cao, Y.; Andreatta, A.; Heeger, A. J.; Smith, P. *Polymer* **1989**, *30*, 2305.
(36) Barbara, T. M.; Gammie, G.; Lyding, J. W.; Jonas, J. *J. Solid State Chem.* **1988**, *75*, 183.
(37) Kumagai, N.; Kumagai, N.; Tanno, K. *J. Appl. Electrochem.* **1988**, *18*, 857.

is a linear function of PANI content up to $x = 0.5$; at $x = 0.25$, only an order of magnitude increase in conductivity compared to the pristine xerogel is observed.[38] In addition, a fraction of the PANI is in the insulating emeraldine base form (as suggested by FTIR, vide supra); this may be due to the only source of protons being that released during polymerization, and the fact that the oxidative coupling process begins outside the layers. We have also found that the minor extent of oxidation of the $MoO_3^{x-}$ layers that occurs during oxidative incorporation of the PANI, which would tend to decrease the conductivity of the inorganic component can be controlled by minimizing the contact of the oxidizing reagent with $A_xMoO_3$.

**B. Electrochemical Lithium Insertion.** The $MoO_3$ host lattice is eminently suitable for Li insertion reactions owing to its layered structure, and therefore it has been proposed as a cathodic material in secondary lithium batteries and electrochromic devices.[20,37,39] Its reported disadvantages are relatively slow kinetics for Li transport, an electronically insulating state when fully oxidized, and poor cycling behavior. The electrochemical insertion of lithium in this material can be described by the following redox couples:

$$MoO_3 + ye^- \rightarrow MoO_3^{y-}$$

$$yLi^+ + MoO_3^{y-} \rightarrow Li_yMoO_3$$

To determine the effect of PANI incorporation between the layers, cells were assembled using the polymer nanocomposite or the alkali bronze as the active cathode material. The open-circuit voltages (OCV) of the two batteries were almost equivalent and comparable to that of a $MoO_3$ thin-film-cathode cell (3.2 V).[20] The chronopotentiometric curves for reduction at a constant current density (60 $\mu$A/cm$^2$ between preset voltage limits of 4.1 and 1.8 V) are shown in Figure 10a for the $[PANI]_{0.24}MoO_3$ cell and in Figure 10b for the $Li_{0.25}MoO_3$ cell. Cycles 1 → 5 are shown in each plot, at a discharge/charge rate of C/12. Electrochemical behavior differs in these two materials, in interesting and significant ways. These can be outlined as follows:

**Cell Polarization.** A significant difference in the degree of polarization in the two cells is apparent, as determined by the magnitude of $\Delta V/2$ between the discharge and charge cycles. It is important to note that the cycling rate was maintained at the same level in both cells, as the rate can affect the polarization when there is a kinetic limitation to Li insertion. We see that, on average, the polarization has decreased by a factor of 1.5−2 in the polymer/oxide nanocomposite (Figure 10a**)** compared to the oxide alone (Figure 10b**)**. The difference between the materials became even more marked on subsquent cycling; i.e., the $[PANI]_{0.24}MoO_3$ cell showed little change in polarization after 10 cycles, whereas polarization in the alkali bronze increased after 10 cycles, especially at low Li mole fraction ($x \sim 0.2$, not shown). This suggests that the effect of the PANI is to enhance Li ion removal from the lattice, especially at low molar fractions of Li, by enhancing either Li ion or electron transport. The difference between the two materials was also reproducible, persisting in all preparations of the alkali bronze or polymer/oxide nanocomposites, and over many different cell assemblies.

**Cell Capacity.** The cell capacity in $[PANI]_{0.24}MoO_3$ *increases* slightly from the first cycle to the second cycle (Figure 10a; 1st reduction sweep vs 2nd reduction sweep) to reach a value of 149 mA h/g at a cycling rate of C/12, compared to 130 mA h/g for $Li_{0.25}MoO_3$.[40] Since the redox potential of the PANI emeraldine salt is similar to that of $MoO_3$, we believe that the modest increase in cell capacity is due, in part, to the incorporation of redox-active poly(aniline). The latter can augment the $MoO_3$ reduction cycle such that additional Li incorporation can take place. This can be thought of in a stepwise sequence, although it is probable that reduction of the PANI and the oxide cannot be isolated in the nanocomposite:

$$[PANI^+]_xMoO_3^{x-} + xLi^+ + xe^- \xleftarrow{\text{reduction of PANI}}$$

$$Li_x[PANI]_xMoO_3^{x-} + yLi^+ + ye^- \xleftarrow{\text{reduction of } MoO_3^{x-}} Li_{x+y}[PANI]_xMoO_3^{-(x+y)}$$

Inclusion of the redox capacity of the PANI, however, only accounts for about 1/2 of the increase in cell capacity; the other component appears to be due to the increase in the kinetics of Li insertion in the PANI nanocomposite. In both materials, we add, the cell capacity is a function of the carbon content which serves as the "inactive" cathode material. There is, therefore, an electronic limitation to electrochemical behavior, despite the presence of the conductive polymer, in accordance with the relatively small degree of enhancement of electronic conductivity that we observed. Future electrochemical studies will concentrate on these factors, in addition to cycling rate dependence, and prolonged cycling times.

**Preservation of Cell Capacity**. For $[PANI]_{0.24}MoO_3$ (Figure 10a) there is only a very small loss in capacity over the first five cycles, indicating near 95% coulombic efficiency for the discharge/charge process. In contrast, for the alkali bronze, the cell capacity drops substantially by about 33% after five cycles (Figure 10b). This is consistent with the known electrochemical behavior of $MoO_3$, which typically shows a sharp decrease in capacity on cycling of up to 40%. The reason for poor cyclability in $MoO_3$ is thought to be the result of irreversible reactions of Li with the lattice, and structural modifications.[41] These appear to be somewhat suppressed on incorporation of the PANI.

(38) Wu, C.-G.; Kanatzidis, M. G. *Mater. Res. Soc. Symp. Proc.* **1991**, *210*, 429.

(39) Pereira-Ramos, J.-P.; Kumagai, N.; Kumagai, N. *J. Power Sources*, **1995**, *56*, 87.

(40) The cell capacity was calculated based on the stoichiometry $[Li_{0.8}Na_{0.2}\cdot 0.8H_2O]_{0.25}MoO_3$, where the water content was determined by TGA analysis of the vacuum-dried (100 °C) material.

(41) Besenhard, J. O.; Schollhorn, R. *J. Power Sources* **1976**, *1*, 267. Besenhard, J. O.; Heydecke, J.; Wudy, E.; Fritz, H. P.; Foag, W. *Solid State Ionics* **1983**, *17*, 21.

(42) Furukawa, Y.; Ueda, F.; Hyodo, Y.; Harada, I.; Nakajima, T.; Kawagoe, T. *Macromolecules* **1988**, *21*, 1297.

(43) Cao, Y.; Li, S.; Xue, Z.; Guo, D. *Synth. Met.* **1986**, *16*, 305.

(44) Cao, Y. *Synth. Met.* **1990**, *35*, 319.

(45) Sotani, N.; Kazuo, E.; Kunitomo, M. *J. Solid State Chem.* **1990**, *89*, 123.

(46) Philip, D.; Aruldhas, G.; Ramakrishnan, V. *Pramaña—J. Phys.* **1988**, *30*, 129.

(47) Milton, A. J.; Monkman, A. P. *J. Phys. D.* **1993**, *26*, 1468.

(48) Barraclough, C. G.; Lewis, J.; Nyholm, R. S. *J. Chem. Soc.* **1959**, 3552.

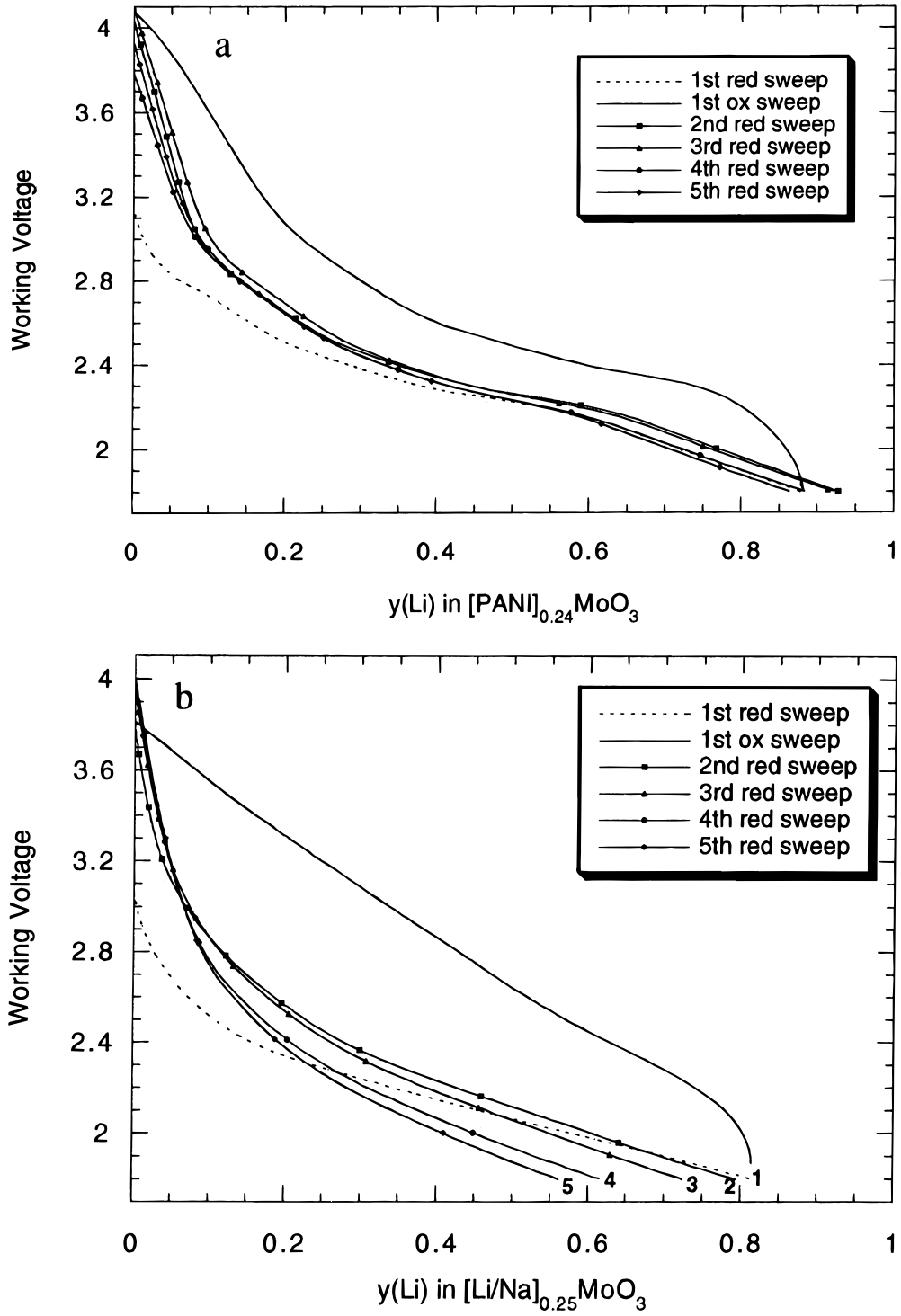


**Figure 10.** Galvanostatic discharge−charge cycling curves of (a) $[PANI]_{0.24}MoO_3$ and (b) $Li_{0.25}MoO_3$.

**Nature of the Reduction Process.** The alkali bronze showed a broad, S-type curve similar to that reported for α-$MoO_3$, in that no well-defined reduction process is apparent from the d*x*/d*V* plot (Figure 11). The reduction process is surprisingly better defined for $[PANI]_{0.24}MoO_3$. Distinct inflections and plateau regions are observed in the discharge−charge curve. The corresponding d*x*/d*V* plot shows three peaks at 2.8, 2.5, and 2.25 V, with the latter being particularly sharp, suggesting that the structure offers more than one type of intercalation site. The lack of kinetic limitation to Li ion transport in the cathode at cycling rates of C/12 is reflected in the high degree of symmetry of the discharge and charge processes. These results suggest that both the molybdenum trioxide and the poly(aniline) are involved in the redox process.

## Conclusions

We have found a novel method of interleaving poly(aniline) between the layers of $MoO_3$ using a low-temperature intercalation technique. This fast reaction is the result of using a concomitant ion exchange−polymerization method in the presence of an external oxidizing agent. The high degree of ordering evident from the oriented film XRD patterns suggests that the

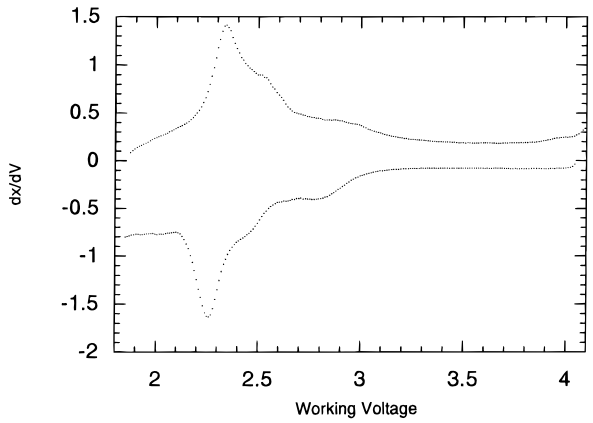


**Figure 11.** d$x$/d$V$ plot for galvanostatic cycling of $[PANI]_{0.24}$-$MoO_3$ at a cycling rate of C/12.

PANI chains are aligned (at least to some degree) in the *ac* (basal) plane.

The nanocomposite displays intriguing effects with respect to electrochemical Li insertion. Despite the relatively small increase in conductivity afforded by incorporation of the polymer, the effect of the polymer is to enhance the battery performance. The presence of the PANI eliminates water from the interlamellar region and can augment the cell capacity due to the additional redox capabilites of the polymer. The results also suggest that the polymer nanocomposite is a better cathode material than the pristine alkali bronze oxide by enhancing lithium diffusion. The oxide groups of the $MoO_3$ bear a partial negative charge and hence strongly attract $Li^+$. This means that a large potential barrier must be surmounted for migration of $Li^+$ from site to site in the lattice, thus hindering the ion mobility. Steric constraints in the 2D gap can also hinder mobility. As a result, diffusion constants for $Li^+$ are quite low in $MoO_3$, on the order of $10^{-11}$–$10^{-12}$ $cm^2$ $s^{-1}$. Our results suggest that the PANI chains have expanded the layers and/or altered the potential surface, hence reducing the polarizability of the lattice.

**Acknowledgment.** LFN gratefully acknowledges the NSERC (Canada) for funding this research through the Research and Strategic grant programs. We thank Professor W. P. Power for acquiring the $^2H$ NMR spectrum and for helpful discussions and R. S. Frank and Prof. M. Gauthier for aiding in the molecular weight determinations. We also thank Molecular Simulations Inc. for the loan of their program Cerius$^2$.

CM960071Q